

Moment-based fatigue load models for wind energy systems

Steven R. Winterstein & LeRoy M. Fitzwater

Department of Civil and Environmental Engineering, Stanford University, Stanford, CA 94305-4020

Lance Manuel

Department of Civil Engineering, University of Texas at Austin, Austin, TX 78712

Paul S. Veers

Sandia National Laboratories, Wind Energy Technology Department, Albuquerque, NM 87185-0708

Keywords: load models, fatigue loads, wind energy, non-Gaussian, moment-based models, long-term, short-term

ABSTRACT: International standards for wind turbine certification depend on finding long-term fatigue load probability distributions that are consistent with respect to the state of knowledge for a given system. Statistical moment-based models of loads for fatigue applications are described and demonstrated here, using flap and edge blade-bending data from a commercial turbine in complex terrain. Distributions of rainflow-counted range data are characterized by a limited number of their statistical moments. Beyond the convenient two-moment (Weibull) model, several higher-moment models are introduced. These include (1) a “quadratic Weibull” model, which uses a quadratic distortion of the original Weibull model to preserve the first three moments of the data; and (2) a “damage-based” Weibull model, which seeks to fit a two-moment model not to the stress ranges themselves, but to a power-law transformation of these that directly reflects “damage” (e.g., based on typical material fatigue properties). The damage-based model is shown to directly follow the tails of the observed data, while the three-moment model also give good tail-fits if the non-damaging low-amplitude ranges are first excluded. Finally, using statistics based on the regression of the relevant moments over the input wind conditions, the uncertainty (due to the limited data set) in the long-term load distribution is represented by a 95% confidence level on predicted loads.

1. INTRODUCTION

Wind energy electrical generation systems have grown in size and complexity at an amazing rate in the last decade. Ten years ago the average size system was less than 20 meters in diameter and generated about 100-200 kilowatts (kW) of electricity in rated winds. Today, machines well over 1 MW in rating and with diameters over 65 meters are on the market, producing electricity for prices below \$0.04/kWh in good wind sites. Machines up to 2.5MW have already been commercially installed and even larger machines are in development, most destined for offshore applications. The total capacity being installed is also increasing exponentially. BTM Consult (a Danish wind energy consulting firm) reports that in 1998 2,600 MW of wind power were installed bringing the worldwide capacity to over 10,000 MW. The following year 3,600 MW of new wind energy generating capacity were installed worldwide, raising total installed capacity over 13,000 MW. Projections are that total installed capacity will easily pass 20,000 MW well before the end of 2002.

This paper is declared a work of the U.S. Government and is not subject to copyright protection in the United States. Sandia National Laboratories is a multi-program laboratory operated by Sandia Corporation, a Lockheed Martin company, for the U.S. Department of Energy under contract DE-AC04-94AL85000.

The ensuing mushrooming capital cost of new product development has driven the industry away from a cut-and-try mentality to a quite sophisticated reliance on numerical simulation and analysis. The design loads are no longer simply scaled up from the last model, but are carefully analyzed to insure an adequate design margin. Fatigue loads are required to be estimated using extreme turbulence levels, intended to envelop the worst measured turbulence levels from around the world. Standards (e.g., IEC/TC88, 1998, 1999) therefore specify analysis at conditions that are easily simulated, but may never be measured on a prototype in the field. Loads must be extrapolated from site conditions to design standard conditions.

Parametric, moment-based models have the ability to describe the reliance of the turbine on the specified turbulence levels by determining the relationship between the governing parameters (moments) of the turbine response and the wind environment (average wind speed V and turbulence intensity I). The fatigue response is characterized by the rainflow counted load ranges R in the response time history. A minimal number of central moments of the rainflow ranges can be used to characterize the distribution of ranges at a given set of inflow conditions. Remaining questions include (1) how many moments are sufficient to predict fatigue damage, which is nonlinearly related to load range amplitude, and (2) how can “higher-moment” models (i.e., including moments of higher than second order) be conveniently constructed?

Here, we present two such higher-moment models: a quadratic Weibull model based on three moments, and a “damage-based” Weibull model based on even higher moments, which are proportional to fatigue damage. The quadratic Weibull model has been previously introduced and applied to other cases of fatigue loads (e.g., Lange, 1996; Veers and Winterstein, 1998; Ronold et al., 1999) and to extreme loads, (e.g., Fitzwater and Winterstein, 2001). In contrast, the damage-based Weibull model is new, suggested here as an alternative that confers certain advantages in some fatigue applications. We demonstrate the use of these models by studying two orthogonal blade-root bending moments: “flap” (out of the plane of blade rotation) and “edge” (in the plane of rotation). The challenges in these cases for the random vibration analyst include the harmonic content of the loads from the rotational motion of the blades, as well as other less easily described nonlinear effects.

The fatigue-load spectra are calculated by splitting the problem into “short-term” and “long-term” aspects. The short-term distribution of load ranges is characterized by operation of the turbine in short (10-minute) quasi-stationary wind conditions (constant average wind speed V and turbulence intensity I). The short-term distribution of load ranges is tied to the relevant statistical moments of the ranges – which, in turn, are related by regression to the input average wind speed and turbulence intensity. Thus, the short-term distribution of ranges may be predicted for any combination of wind conditions.

The long-term distribution of ranges is then easily obtained by integrating over the joint annual distribution of input conditions. As another benefit of the parametric, moment-based, load models, we show how standard uncertainty results from the regression-fit moments can be used to directly quantify the uncertainty (due to the limited data set) in the long-term fatigue load distribution. Specifically, we show how a 95% confidence load level on this distribution can be found from these limited data, and how these differ from “deterministic” results that ignore this uncertainty.

2. EXAMPLE DATA SET

An example data set taken from the copious measurements of the MOUNTURB program (MOUNTURB, 1996) is used to illustrate the parametric modeling process. The data are comprised of 101 ten-minute samples of rainflow-counted flap-wise and edge-wise bending-moment ranges at the blade root. The test turbine is a WINCON 110XT, a 110kW stall-regulated machine operated by CRES (the Centre for Renewable Energy Systems, Pikermi, Greece) at their

Lavrio test site about 50 km southeast of Athens. The terrain is characterized as “complex,” meaning irregular enough to produce significant atmospheric turbulence.

The original time series of the loads and winds were not available for further analysis; thus, only the rainflow-counted ranges were employed. The number of cycle counts was tallied in 50 bins ranging from zero to the maximum range in each sample. A single ten-minute sample is categorized by the mean wind speed and the raw turbulence intensity at hub height. The average wind speeds are limited to the range between 15 and 19 m/s and thus reflect response in high wind operation. Turbulence intensities cover a wide range of operating conditions as can be seen in Figure 1. The measured loads are summarized by frequency of occurrence in Figure 2a for flap moment ranges and in Figure 2c for edge moment. Plots showing exceedance counts for specified flap and edge loads are shown in Figures 2b and 2d, respectively. The “histograms” in Figures 2a

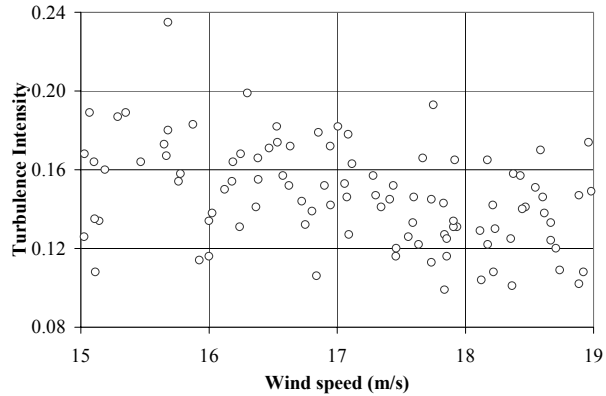


Figure 1: Wind speed and turbulence intensity values for the 101 10-minute data samples.

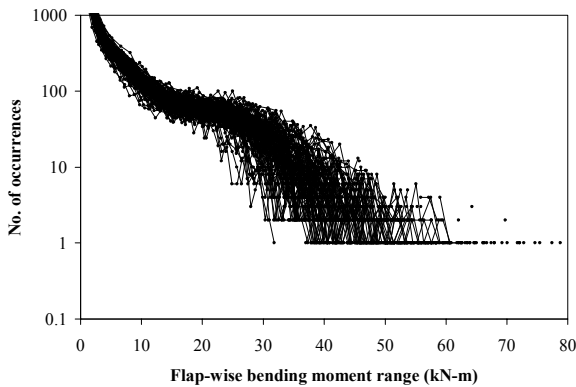


Figure 2a: Histogram of flap-wise bending moment ranges for 101 10-minute data sets.

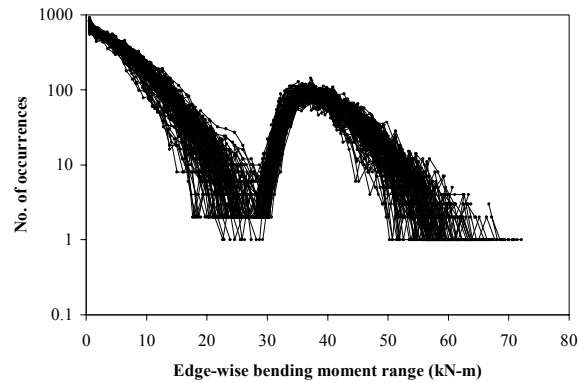


Figure 2c: Histogram of edge-wise bending moment ranges for 101 10-minute data sets.

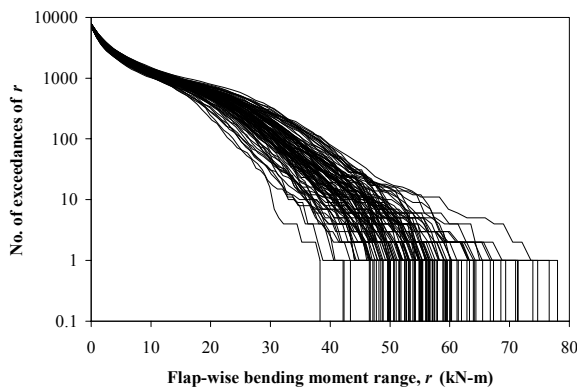


Figure 2b: Cumulative counts of flap-wise bending moment ranges for 101 10-minute data sets.

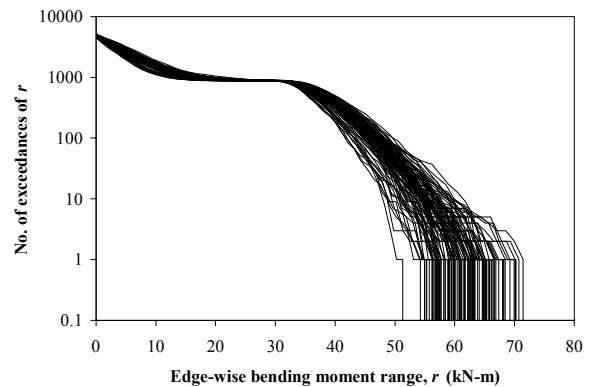


Figure 2d: Cumulative counts of edge-wise bending moment ranges for 101 10-minute data sets.

and 2c show the number of counts in each finite width bin of bending moment range. Notice that the minimum number of counts in any given bin is one. The exceedance curves are shown going to zero at the largest measured range.

3. SHORT-TERM ANALYSIS

We assume here that the stress response of the wind turbine remains stationary within each 10-minute duration event. To predict fatigue damage in such an event, it is common to assume that a single stress range R produces damage $D \propto R^b$. (b is a material constant from fatigue test data, where the number of constant-amplitude cycles to failure is assumed proportional to R^{-b} .)

The Standard Weibull Model. A conventional approach is to model an arbitrary stress range, R , as a random variable, $W=R$, with Weibull probability distribution function:

$$P[W > x] = \exp\left[-(x/\alpha_W)^{\beta_W}\right]. \quad (1)$$

The corresponding statistical moments of W are given by

$$E[W^b] = \alpha_W^b (b/\beta_W)!. \quad (2)$$

In practice, one estimates the first two range moments from the data, and uses Eq. 2 with $b=1$ and 2 to infer the parameter values of α_W and β_W . The mean damage per cycle, $E[D] \propto E[R^b]$, is also found directly from Eq. 2 for arbitrary b .

There are two main benefits of this Weibull model. First, it requires relatively little data; specifically, data sufficient only for accurate prediction of the first two moments of the stress ranges. Second, the closed-form moment results facilitate both the parameter fitting of α_W and β_W from the data, and the consistent estimation of $E[D]$ from α_W and β_W .

The simple two-moment characterization of the Weibull model is also its potential drawback. Typical b values for metals may range from 3 to 8, with lower values more typical for welded steels and higher values for aluminum. As b increases, $E[D] \propto E[R^b]$ becomes increasingly sensitive to the details of the stress range distribution in its upper tail. Any deviation from the Weibull model in this upper region can lead to erroneous damage predictions. Composites often show still higher b values – e.g., $b=10$ or higher – and hence give still larger potential for the two-moment Weibull model to err. We describe here two models that seek to address these potential modeling errors, through the use of higher-order statistical moments.

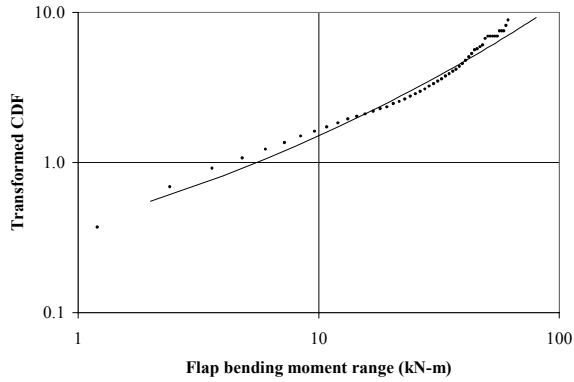
Approach 1: Quadratic Weibull Model. The quadratic Weibull model again starts with a Weibull variable W , whose parameters α_W and β_W are chosen to preserve the first two range moments. A quadratic perturbation term is then added to better model the actual range R :

$$R = R_0 + \kappa[W + \varepsilon W^2] \quad (3)$$

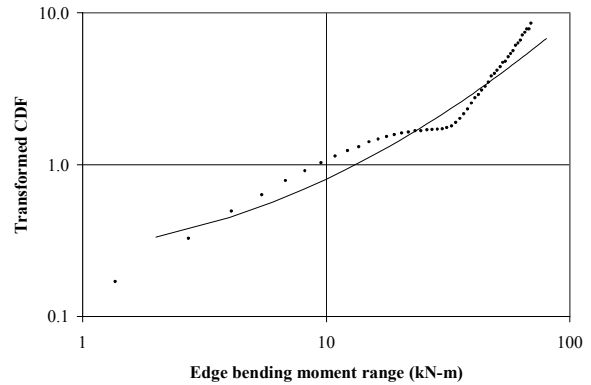
The coefficient ε is chosen here so that the skewness (third normalized moment) of the range data is preserved. The remaining parameters, κ and R_0 , are finally chosen to preserve the variance and mean of R respectively. (Note that Eq. 3 is applied directly only when the skewness of R is found to exceed that of the Weibull variable W . In this case, the quadratic term εW^2 serves to enhance the skewness, from that of the Weibull variable to that of the observed ranges. If the skewness of R is instead found to be less than that of W , the roles of R and W in Eq. 3 are interchanged.) Additional technical details can be found in Lange (1996) and Manuel, et al. (1999). Other applications of this model to fatigue loads can be found in Ronold, et al. (1999) and Manuel, et al. (2001), and to extreme loads in Fitzwater and Winterstein (2001).

Thus, the resulting quadratic Weibull distribution of R preserves the first three statistical moments of the data. Its distribution function appears as a quadratic curve when plotted on Weibull probability scale. To illustrate, Figures 3-4 show range results from one of the 101 measured samples. This data sample is taken from the middle of the measured wind conditions: $V=17$ m/s and $I=0.18$. The data are plotted on a Weibull scale for the flap data in Figure 3 and for the edge loads in Figure 4. These plots transform the vertical scale by plotting not the cumulative distribution $F(r)=P[R<r]$ but rather $-\ln[1-F(r)]$, so that the Weibull distribution will appear as a straight line on a log-log plot.

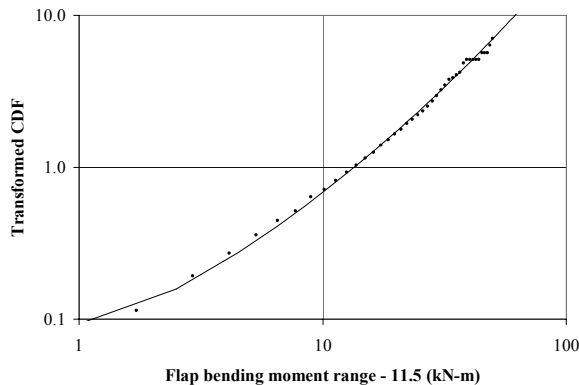
Figures 3a and 4a show attempts to fit the entire flap and edge data with quadratic Weibull models. As seen in Figure 3a and especially Figure 4a, the data have a kinked appearance which the smooth probability distribution, in spite of its quadratic distortion, has difficulty matching. Closer examination of the data reveals that the kink is due to a very large number of cycles at relatively low amplitudes. By truncating the loads at a lower-bound threshold, however, the kink in the data can be eliminated without significantly reducing damage. In the edge case, there are obviously a great number of cycles of smaller amplitude than the dominant gravity load at about 32 kN-m. The flap loads have a less distinctive kink at around 10-13 kN-m (11.5 kN-m was used as the filtering threshold). Figures 3b and 4b are similar to Figures 3a and 4a, but include only a subset of the data by removing all ranges beneath a lower-bound threshold R_{th} , and modeling the



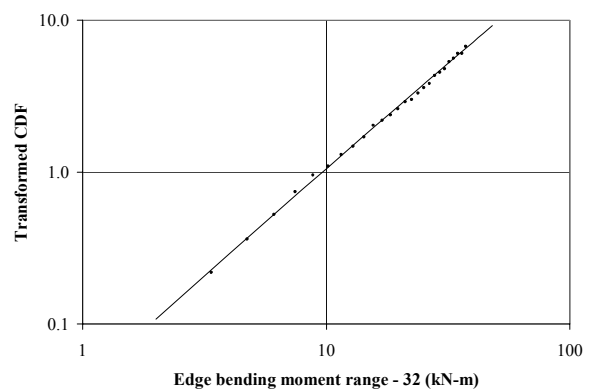
(a) Weibull scale plot, all data and fit.



(a) Weibull scale plot, all data and fit.



(b) Weibull scale plot (truncation at $R_{th}=11.5$ kN-m and shifted by $R-R_{th}$.)



(b) Weibull scale plot (truncation at $R_{th}=32.0$ kN-m and shifted by $R-R_{th}$.)

Figure 3: Quadratic Weibull model fits to flap-bending moment ranges ($V=17.0$ m/s, $I=0.18$).

Figure 4: Quadratic Weibull model fits to edge-bending moment ranges ($V=17.0$ m/s, $I=0.18$).

shifted variable $R-R_{th}$ with our (positively valued) quadratic Weibull model. Clearly, the fits of the quadratic Weibull are improved dramatically. It has also been shown (Manuel et al, 2001) that the damage omitted through the use of this threshold is negligible in this case, which is consistent with findings that have long been available in the fatigue literature (e.g., Nelson and Fuchs, 1977).

In summary, the quadratic Weibull model offers the ability to match the first three moments of the data set. The resulting quadratic behavior of its distribution function, on Weibull scale, can yield an excellent fit to stress range data (e.g., the flap data in Figure 3b). In other cases, a simpler linear/Weibull model may suffice (e.g., the edge data in Figure 4b). The main drawbacks of the quadratic Weibull model are that (1) simple closed-form moment results are no longer available, so that parameter estimation must be performed numerically; and (2) the analyst may need to first impose a lower-bound threshold to exclude uninteresting, small-amplitude ranges. Neither of these problems is insurmountable; indeed, numerical algorithms are available to facilitate the use of these higher-moment models (e.g., Manuel et al, 1999). However, we explore next an alternative, “damage-based” Weibull model that is somewhat simpler to implement.

Approach 2: Damage-Based Weibull Model. As noted earlier, the damage per cycle is commonly related to R^b , the b^{th} power of the stress range R . Because typical b values far exceed unity, standard second-moment Weibull fits may not accurately predict the higher moment $E[R^b]$ that drives damage accumulation.

Our proposed damage-based Weibull model notes that if R follows a Weibull distribution, the power-law transformation R^z , where z is an arbitrary power on the ranges, also follows a (modified) Weibull distribution. We therefore use a second-moment Weibull fit not of the range R , but rather an associated variable

$$W=R^z. \quad (4)$$

By choosing $z=b/2$, and matching the second moment of the resulting distribution of W , the damage potential of the range distribution for a given material (where b is the slope of the $S-N$ curve) is preserved.

For example, with $z=3$ this Weibull fit will preserve both $E[R^3]$ and $E[R^6]$, which are typical for some welded steels ($b=3$) and aluminums ($b=6$), respectively. For wind turbine applications, even higher moments are of interest because fiberglass composite blades possess b values equal to 8, 10, or even higher.

In practice, the damage-based Weibull model is fit by (1) transforming the range data R through Eq. 4, (2) using a standard second-moment fit for the Weibull parameters α_W and β_W ; and (3) plotting the resulting distribution function, $F(w)$, versus not w but rather $r=w^{1/z}$. The benefits of this model are that (1) it requires only a standard second-moment Weibull fitting procedure, easily implemented without specialized algorithms; and (2) it explicitly ensures accurate distribution modeling in the range most relevant for damage prediction; i.e., in the upper tail of the stress range distribution. (A similar upper tail fit model can be used to predict ultimate loads as well, although in this case there is no physical motivation for a particular choice of $b=2z$ value.)

Figures 5a and 5b repeat the Weibull scale distribution plots of all data for flap and edge loads, respectively, for one 10-minute sample. Also shown on these figures are three damage-based Weibull predictions, which utilize the parameter choices $z=3, 4,$ and 5 . (A choice of $z=5$ may be more appropriate for wind turbine blades, preserving the $b=10^{\text{th}}$ moment which may govern damage of these composite components.) As may be expected, these models provide accurate load distribution estimates in the upper tail of interest. (Increasing z values leads to enhanced emphasis on the upper tail.) Note again the advantages of these models, by permitting tail-fitting in an automated, physically-based way. They also avoid the need to impose a lower-bound load threshold; all ranges may be included, and the original cycle rate preserved. Of course, the damage-based Weibull model, because it emphasizes upper-tail behavior, will provide a poor estimate of low-fractile loads, but these loads have little or no effect on damage prediction.

4. LONG-TERM ANALYSIS

To review, the load models proposed here estimate the probability distribution of load ranges, R , by preserving a limited set of statistical moments, $\mu_n = E[R^n]$. The relevant moments here are model-dependent: μ_1 and μ_2 are used for the standard Weibull model, μ_1 through μ_3 for the quadratic Weibull model, and μ_z and μ_{2z} for the damage-based Weibull model (z on the order of 3-5, $b=6-10$). Finally, regression analysis is used to relate each moment μ_n to the mean wind speed, V , and turbulence intensity, I , through a power-law relation:

$$\mu_n = a_n \left(\frac{V}{V_{ref}} \right)^{b_n} \left(\frac{I}{I_{ref}} \right)^{c_n} \quad (5)$$

Hence, for these parametric load models, the wind turbine characteristics are reflected solely through the moment relations in Eq. 5. For example, with the quadratic Weibull model we require the 9 coefficients a_n, b_n, c_n ($n=1, 2, 3$) that govern the first three range moments. For clarity, we organize these coefficients here into a vector, denoted θ :

$$\theta = [a_1, b_1, c_1, a_2, b_2, c_2, a_3, b_3, c_3] \quad (6)$$

The other (standard or damage-based) Weibull models require only two moments, and hence 6 coefficients in the vector θ . Linear regression analysis, applied to the logarithm of Eq. 5, yields point estimates of these coefficients, together with uncertainty levels (standard error estimates) due to the limited data available. Manuel et al. (2001) report these regression results for the 9 coefficients in Eq. 6. To demonstrate typical results we pursue only the quadratic Weibull model here, although the alternate, damage-based Weibull model may also be used for this purpose. (One should expect somewhat larger uncertainties to arise from these damage-based models, in view of their effective tail-fitting procedures.)

The long-term distribution of fatigue load ranges is found by integrating the short-term load range distribution, $F(r|V, I, \theta)$, over the probability density $f(V)$ associated with different wind speeds V :

$$F(r|\theta) = \int F(r|V, I, \theta) f(V) dV \quad (7)$$

For a particular wind speed V , the associated turbulence intensity I is chosen here as the conditional mean of I (given V) for the Lavrio site. Site-specific uncertainty in I given V can also be included, replacing Eq. 7 by a double integration over both I and V . Notably, using the mean

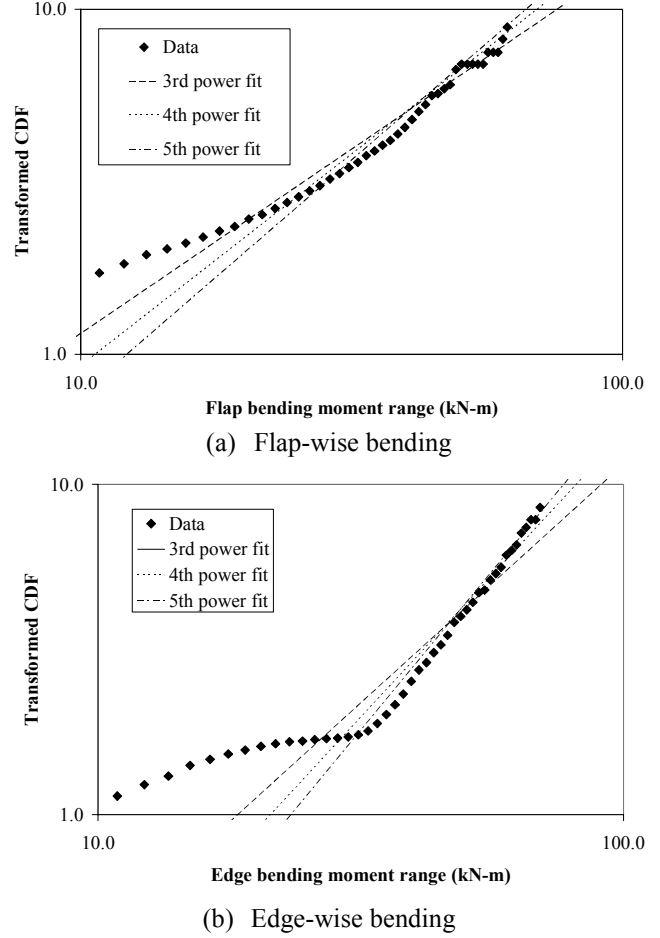
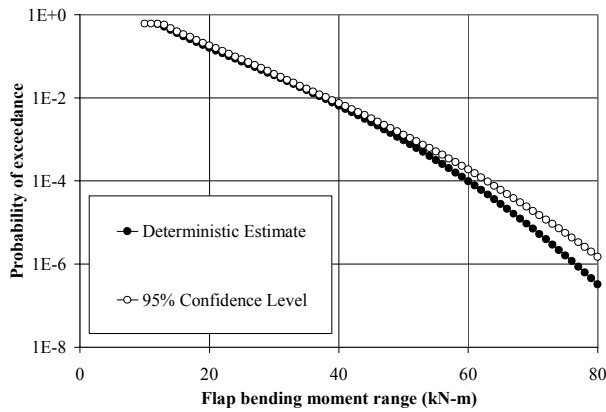
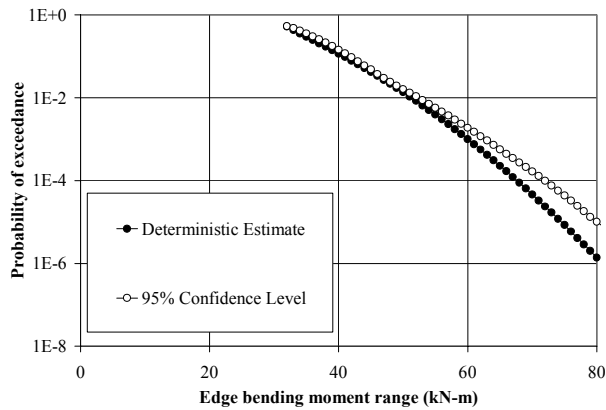


Figure 5: Damage-based Weibull model fit to blade root bending ranges ($V=17.0$ m/s, $I=0.18$).



(a) Flap-wise bending



(b) Edge-wise bending

Figure 6 95% Confidence levels on the exceedance probability of fatigue loads for the Lavrio site with turbulence set to the average value for each wind speed.

and (3) sort the resulting $F(r)$ values (at each fixed r value) to establish a confidence level below which 95% of all loads will lie.

Figures 6a and 6b show the 95% confidence level on the exceedance probability, $1-F(r)$, which result from the simulation procedure described above. Each of the 9 coefficients in Eq. 6 were generated as statistically independent, normally distributed random variables, with means and standard deviations estimated by standard linear regression techniques (e.g., Manuel et al, 2001). (Correlation among these variables can also be included; however, this was not done here.)

In addition to the 95% confidence results, Figures 6a and 6b also show “deterministic” results, constructed by ignoring the uncertainty in the regression-based estimators. The increase in probability of exceedance over the deterministic results in order to achieve 95% confidence is found to be relatively modest in the body of the distribution, but begins to be significant at very high load ranges. This reflects the benefit of having as many as 101 10-minute samples that can clearly establish average behavior, while the extremes retain a fairly high uncertainty even with large data sets. If the same mean trends had resulted from fewer samples, the resulting 95% confidence results would be considerably higher than the mean (or deterministic) results. Finally,

value of turbulence has been found conservative for this particular turbine and site due to the reduced turbine loading when the turbulence levels are low (Manuel et al., 2001).

Because Eq. 7 expresses the long-term load distribution in terms of a limited set of (nine) coefficients, contained in θ , it provides a useful means by which to estimate the effects of limited data. To clarify, it is useful to distinguish between the various terms in Eq. 7. The quantities V and I are “random variables;” that is, their future outcomes will show an intrinsic randomness that cannot be reduced by additional study of past wind conditions. In contrast, the 9 coefficients in θ are in principle fixed (under the model’s assumptions). We will typically, however, be uncertain as to their precise values due to limited response data. This “uncertainty” (as opposed to “randomness”) can be reduced through additional sampling. The consequence of having only limited data can be reflected by determining the 95% confidence levels, for example, on the exceedance probability $1-F(r)$.

Confidence levels are conceptually straightforward to establish by simulation. Assuming the entries of θ to each be normally distributed, for example, one may (1) simulate multiple outcomes of θ ;

(2) estimate $F(r)$ for each θ as in Eq. 7;

we caution again that these long-term load results are intended for example purposes only; accurate numerical values would require data across a broader range of wind speeds.

5. SUMMARY

Parametric, moment-based, statistical models have been introduced to model rainflow-counted fatigue ranges. Two “higher-moment” models (including third and/or higher moments) have been presented: (1) a quadratic Weibull model, which uses a quadratic distortion of the original Weibull model to preserve the first three moments of the data; and (2) a “damage-based” Weibull model, which seeks a two-moment Weibull fit, not to the stress ranges themselves but to power-law transformations that directly relate to “damage” (i.e., based on material properties defining S-N curve slope, b). Both models have their advantages. Compared with measured fatigue load data, the “damage-based” Weibull model is found to directly follow the tails of the observed data (as seen, for example, in Figure 5). It also requires no special numerical algorithms to estimate its parameters. In contrast, the quadratic Weibull does require such algorithms, and its accurate modeling of distribution tails can require the analyst to impose a lower-bound threshold on the load ranges to be modeled (see Figures 3a and 4a versus Figures 3b and 4b). The potential benefit of the quadratic Weibull model includes its reliance only on moments through third order. The damage-based model requires moments of order $z=b/2$, where typical z values may range from 3 to 5 reflecting material properties $b=6-10$. Hence, to the degree it remains accurate, the quadratic Weibull model can be fit more accurately from limited data. We have also shown the effects of having such limited data, by propagating statistical uncertainty (in the requisite moments) to establish 95% confidence levels on the long-term fatigue loads distribution (Figure 6). For the example data from Lavrio, the increase in 95% confidence level probability over the deterministic estimates is relatively modest except in the tails where the uncertainty remains high. These results also show the convenience of the moment-based models in creating these 95% confidence level results: statistical uncertainty in the requisite moments is directly quantified by standard regression techniques, as a function of wind input conditions.

6. ACKNOWLEDGMENTS

The authors would like to extend a special debt of gratitude to the Centre for Renewable Energy Sources (CRES), Pikermi, Greece and especially to Fragiskos Mouzakis who found time in a busy schedule to supply the portion of the MOUNTURB data set used in the examples.

REFERENCES

- IEC/TC88, 61400-1 1998. *Wind Turbine Generator Systems – Part 1: Safety Requirements*, International Electrotechnical Commission (IEC), Geneva, Switzerland,
- IEC/TC88, 1999. *Draft IEC 61400-13 TS, Ed. 1: Wind turbine generator systems – Part 13: Measurement of mechanical loads*, 88/120/CDV, International Electrotechnical Commission (IEC), Geneva, Switzerland.
- Fitzwater, L. M. and Winterstein, S. R., 2001. “Predicting Design Wind Turbine Loads from Limited Data: Comparing Random Process and Random Peak Models,” *A collection of the 2001 ASME Wind Energy Symp., at the AIAA Aerospace Sciences Mtg.*, Reno, Nevada, AIAA-2001-0046.
- Lange, C. H., 1996. *Probabilistic Fatigue Methodology and Wind Turbine Reliability*, SAND96-1246, Sandia National Laboratories, Albuquerque, NM.
- Manuel, L., Veers, S. P., and Winterstein, S. R., 2001. *Parametric Models for Estimating Wind Turbine Fatigue Loads for Design*, *A collection of the 2001 ASME Wind Energy Symp., at the AIAA Aerospace Sciences Mtg.*, Reno, Nevada, AIAA-2001-0047.

- Manuel, L., Kashef, T. and Winterstein, S. R., 1999. *Moment-Based Probability Modelling and Extreme Response Estimation The Fits Routine, Version 1.2*, SAND99-2985, Sandia National Laboratories, Albuquerque, NM.
- MOUNTURB 1996. *Load and Power Measurement Program on Wind Turbines Operating in Complex Mountainous Regions*, Volumes. I - III, Editor P. Chaviaropoulos, Coord. A. N. Fragoulis, CRES, RISO, ECN, NTUA-FS, published by CRES, Pikermi, Greece.
- Nelson, D. V., and Fuchs, H. O., 1977. "Predictions of Cumulative Fatigue Damage using Condensed Load Histories," *Fatigue under Complex Loading: Analysis and Experiments, Advances in Engineering*, Vol. 6, Ed. R. M. Wetzel, SAE, Warrendale, PA.
- Ronold, K. O., Wedel-Heinen, J. and Christensen, C. J., 1999. "Reliability-based fatigue design of wind-turbine rotor blades," Elsevier, *Engineering Structures* 21.
- Veers, P. S. and Winterstein, S. R., 1998. "Application of Measured Loads to Wind Turbine Fatigue and Reliability Analysis," *Journal of Solar Energy Engineering, Trans. of the ASME*, Vol. 120, No. 4.